

NLTE models of line-driven stellar winds

II. O stars in SMC

Jiří Krtička[†]

Ústav teoretické fyziky a astrofyziky PřF MU, CZ-611 37 Brno, Czech Republic

Received

ABSTRACT

We calculate NLTE line-driven wind models of selected O stars in the spectral range of O4 to O9 in the Small Magellanic Cloud (SMC). We compare predicted basic wind properties, i.e. the terminal velocity and the mass-loss rate with values derived from observation. We found relatively good agreement between theoretical and observed terminal velocities. On the other hand, predicted mass-loss rates and mass-loss rates derived from observation are in a good agreement only for higher mass-loss rates. Theoretical mass-loss rates lower than approximately $10^{-7} M_{\odot} \text{ year}^{-1}$ are significantly higher than those derived from observation. These results confirm the previously reported problem of weak winds, since our calculated mass-loss rates are in a fair agreement with predictions of Vink et al. (2001). We study multi-component models for these winds. For this purpose we develop a more detailed description of wind decoupling. We show that the instability connected with the decoupling of individual wind elements may occur for low-density winds. In the case of winds with very low observed mass-loss rate the multicomponent effects are important for the wind structure, however this is not able to consistently explain the difference between predicted mass-loss rate and mass-loss rate derived from observation for these stars. Similar to previous studies, we found the dependence of wind parameters on the metallicity. We conclude that the wind mass-loss rate significantly increases with metallicity as $\dot{M} \sim Z^{0.67}$, whereas the wind terminal velocity on average depends on metallicity only slightly, namely $v_{\infty} \sim Z^{0.06}$ (for studied stars).

Key words: stars: winds, outflows – stars: mass-loss – stars: early-type – hydrodynamics – instabilities – galaxies: Magellanic Clouds

1 INTRODUCTION

In recent few years 8m class telescopes became routinely available for the stellar research. This enabled detailed study of many stars in the Local Group. Clearly, many astrophysically important types of stars can be studied from another perspective. This is especially true for stars from the Small Magellanic Cloud (SMC). Their lower metallicity compared to the solar value (the average metallicity of individual elements is $Z/Z_{\odot} = 0.2$, e.g. Venn 1999, Bouret et al. 2003) enables to study the stellar properties and evolution with respect to metallicity.

One of the most important properties of hot stars, that can influence both the observed spectrum and the stellar evolution, is the presence of the stellar wind. The existence of significant dependence of the basic wind properties (i.e. the amount of mass expelled from the star per unit of time, the mass-loss rate and the wind velocity at large distances from the star, the terminal velocity) on the metallicity has been anticipated already at the very beginning of the theoretical study of hot star winds (Abbott 1982, Kudritzki et al. 1987). Although the most abundant elements in the observed uni-

verse, hydrogen and helium mostly contribute to the wind density, their contribution to the radiative acceleration is very small (e.g. Abbott 1982). Heavier elements like carbon, nitrogen, oxygen or iron are much more important for the wind acceleration of present hot stars. This is because heavier elements have effectively much more lines that are available to absorb the stellar radiation and to accelerate the stellar wind. Clearly, in most cases the radiative force shall be higher for higher metallicity. Consequently, the basic wind properties shall depend on the metallicity.

Although relatively simple expressions for the dependence of the mass-loss rate and the terminal velocity on the metallicity can be obtained even on the basis of the standard CAK (Castor, Abbott & Klein 1975) theory (e.g. Puls et al. 1998), the detailed dependence is probably more complicated (Puls et al. 1998, Vink et al. 2001). It is clear that more precise (NLTE) wind models are necessary to study this problem in detail.

There are several independent NLTE wind models that can be used for the study of the metallicity dependence of the wind properties. These codes differ in the level of sophistication of the treatment of the wind problem. One of the most important aspects that influences the reliability of individual NLTE wind models is the inclusion of proper bound-free and bound-bound blanketing in

[†] E-mail: krticka@physics.muni.cz

the UV domain. While models of Vink et al. (2001, hereafter VKL) use Monte Carlo method for the solution of the radiative transfer equation, models of Pauldrach et al. (2001) solve this equations in detail. Wind models of Gräfener & Hamann (2005), that were successfully used for the calculation of wind models of WR stars, use comoving-frame formulation of the radiative transfer equation. All these models to some extent properly take into account blanketing effects in the UV domain that are important for the correct calculation of the ionization balance and of the radiative force. Hence, these models are able to reliably predict the most important wind parameter – the mass-loss rate and its metallicity dependence.

However, also the wind velocity field and especially the terminal velocity can be influenced by the metallicity. To study this effect, the solution of hydrodynamic equations is necessary. Since models of VKL, that are widely used in hot star evolutionary calculations, do not solve these equations, these models assume a pre-specified velocity law and cannot be used for the predictions of the velocity structure. This is an important difference between models of VKL and e.g. Pauldrach et al. (2001) or Gräfener & Hamann (2005). Hydrodynamical wind models for different metallicities were calculated by Kudritzki (2002). According to these models the wind terminal velocity decreases with decreasing metallicity, in agreement with SMC observations (see an extensive compilation of Kudritzki & Puls 2000).

However, the wind metallicity does not vary the radiative force only. The momentum acquired by the heavier elements from the radiative field is transferred to the bulk wind component (i.e. hydrogen and helium) via the Coulomb collisions. Since the frictional force caused by these collisions depends on number densities of heavier elements and hydrogen-helium component, the effects induced by the collisions are more important in the low-metallicity environment (Kudritzki 2002, Krtička et al. 2003). NLTE models available to study this problem were presented by Krtička & Kubát (2004, hereafter KK1).

Some hot stars with low luminosities (and consequently low mass loss rates) show signatures of very weak winds, much weaker than that deduced from standard wind theory (Bouret et al. 2003; Martins et al. 2004; 2005). Since this discrepancy is based mostly on wind models of Vink et al. (2001), it would be interesting to test this result also with independent NLTE wind models and to test whether this discrepancy can be caused by multicomponent effects.

The study of the metallicity dependence of stellar wind properties is not important only for our understanding of stellar winds or massive stars itself. Since stellar winds play a role in the chemical enrichment of galaxies and are responsible for input of a large amount of momentum and energy in the interstellar medium, the detailed knowledge of variations of basic wind parameters with metallicity is important also for other fields of astrophysics.

As we have discussed, wind properties of hot stars shall depend on the stellar metallicity. Low-metallicity environment of SMC offers a unique possibility to test these available predictions. To do so, we present here wind models for selected SMC hot stars.

2 MODEL DESCRIPTION

The models applied in this paper were in detail described by KK1. Here we only summarise the basic model properties and refer an interested reader to this paper.

Models assume spherically symmetric and stationary stellar wind. Occupation numbers of selected atoms and ions (see Table 1) are obtained by the solution of statistical equilibrium (NLTE)

Table 1. Atoms and ions included in the NLTE calculations. In this table, level means either an individual level or a set of levels merged into a super-level.

Ion	Levels	Ion	Levels	Ion	Levels
H I	9	Ne IV	12	S IV	18
H II	1	Ne V	17	S V	14
He I	14	Ne VI	1	S VI	16
He II	14	Na II	13	S VII	1
He III	1	Na III	14	Ar III	25
C II	14	Na IV	18	Ar IV	19
C III	23	Na V	16	Ar V	16
C IV	25	Na VI	1	Ar VI	1
C V	1	Mg II	14	Ca II	16
N II	14	Mg III	14	Ca III	14
N III	32	Mg IV	14	Ca IV	20
N IV	23	Mg V	13	Ca V	22
N V	13	Mg VI	1	Ca VI	1
N VI	1	Al III	14	Fe III	29
O II	50	Al IV	14	Fe IV	32
O III	29	Al V	1	Fe V	30
O IV	39	Si III	12	Fe VI	27
O V	14	Si IV	13	Fe VII	1
O VI	20	Si V	15	Ni III	36
O VII	1	Si VI	1	Ni IV	38
Ne II	15	S II	14	Ni V	48
Ne III	14	S III	10	Ni VI	1

equations together with the radiative transfer equation. The radiative transfer equation in lines is solved in the Sobolev approximation (Sobolev 1947, Castor 1974), whereas the continuum radiative transfer equation is solved by Feautrier method in the spherical coordinates (see Mihalas & Hummer 1974 or Kubát 1993). Derived occupation numbers are used to calculate the radiative force (in the Sobolev approximation) and the radiative cooling/heating term (using the thermal balance of electrons method, Kubát et al. (1999)). This enables to solve the hydrodynamic equations. These procedures are iterated to obtain consistent model structure. Finally, wind mass-loss rates and terminal velocities of studied stars can be obtained from our models and compared with observations.

Although our models involve some simplifying assumptions (especially the simplified treatment of the radiative transfer (splitting of the radiative transfer in continuum and in the lines, neglect of line overlaps) compared to more advanced models of e.g. Pauldrach et al. (2001), VKL or Gräfener & Hamann (2005)), they were able to correctly predict basic wind parameters of late O stars (see KK1) and of A supergiant (see Krtička & Kubát 2004). Moreover, our models have some advantages compared to some other models available in the literature, for example the direct calculation of the radiative force without using of force multipliers or multicomponent treatment of model equations (see Krtička & Kubát 2001, hereafter KKII).

Presented models were only slightly modified with respect to the status described by KK1. First, we included accelerated lambda iterations in continuum (or, more precisely, approximate Newton-Raphson iterations) based on Rybicki & Hummer (1992) paper and Ng acceleration (Ng 1974) to accelerate the convergence of the system of statistical equilibrium equations (see also Hillier & Miller (1998), or Hubeny (2003) for a review). This will be described in a following paper (Krtička & Kubát, in preparation). Second, our previous set of included atomic models based on TLUSTY files (Hubeny 1988, Hubeny & Lanz 1992, Hubeny & Lanz 1995, Lanz

& Hubeny 2003) or Opacity Project (Seaton 1987, Luo & Pradhan 1989, Sawey & Berrington 1992, Seaton et al. 1992, Butler et al. 1993, Nahar & Pradhan 1993) and Iron Project (Hummer et al. 1993, Bautista 1996, Nahar & Pradhan 1996, Zhang 1996, Bautista & Pradhan 1997, Zhang & Pradhan 1997, Chen & Pradhan 1999) data was slightly extended (see Table 1). These mentioned changes do not significantly influence the derived results. To complete the list of atomic databases used, the oscillator strengths necessary for the calculation of the radiative force are extracted from the VALD database (Piskunov et al. 1995, Kupka et al. 1999).

The boundary radiative flux is taken from grid of line-blanketed plane-parallel model atmospheres OSTAR2002 (Lanz & Hubeny 2003) instead of from H-He spherically symmetric models of Kubát (2003). Since line-blanketed fluxes have generally lower flux in the UV region (where are many lines important for radiative driving), obtained mass-loss rates are slightly lower (roughly $1.4 \times$) than that derived using H-He fluxes. However, this difference is lower than the dispersion of mass-loss rates for Galactic O stars (see KK1) and does not significantly influence predicted wind terminal velocities (the difference between the terminal velocities is about 100 km s^{-1}).

3 CALCULATED WIND MODELS

3.1 Parameters of studied SMC stars

Since our main intention for future studies is to study weak winds of B stars, for the present study we selected only those cooler (i.e. with effective temperatures $T_{\text{eff}} \lesssim 42\,000 \text{ K}$) O SMC stars, for which at least reliable estimate of their mass-loss rate is available in the literature. We tried to omit those stars for which their wind parameters are uncertain and which are binaries. Moreover, we also aim to base the list on broader surveys with larger number of individual stars studied. Stellar parameters and wind parameters of these stars are given in Tab. 2. Stellar effective temperatures and radii are taken from Puls et al. (1996, hereafter P96), Bouret et al. (2003, hereafter B03) and Massey et al. (2004, hereafter M04). Whereas parameters given by P96 were obtained by models without wind-blanketing, parameters given by B03 and M04 were derived using models with wind-blanketing. To study the thin-wind problem in detail we added also stars from Martins et al. (2004, hereafter Mr04) sample. These stars are suspected Vz stars, i.e. stars close to the ZAMS. They exhibit much lower wind spectral signature than that predicted from standard theory. On the other hand there are only upper limits of their observed mass-loss rates and lower limits of their observed terminal velocities available.

SMC stars are in some sense more suitable for the test of theoretical models than stars from our Galaxy. Since the distance to SMC is known with relatively high precision, the stellar radius and mass-loss rate may be also derived more reliably.

For our study we adopted evolutionary stellar masses either derived by B03 or by us using evolutionary tracks of stars with initial metallicity $Z/Z_{\odot} = 0.2$ calculated by Charbonnel et al. (1993). The use of the evolutionary masses is a relatively important assumption that can significantly influence the results derived due to the discrepancy between stellar masses of hot stars derived from evolutionary tracks and from spectroscopy (Herrero et al. 1992). Since KK1 in their analysis used evolutionary masses, we also use evolutionary masses here, but in fact for many stars from KK1 sample these masses are nearly equal. Our SMC sample is not homogeneous in that sense, since for some stars these masses are equal,

but for a significant part of stars the evolutionary mass is roughly $1.5 \times$ higher than the spectroscopic one. The use of spectroscopic masses instead of the evolutionary ones would help to obtain a better agreement between observation and theory for some stars, however it would cause differences for some others.

When available, the abundances of individual elements were taken from the literature, however in other cases we assumed average value $Z/Z_{\odot} = 0.2$ derived for SMC stars (e.g. Venn 1999, M04). We use Galactic helium abundance.

There are indications that stellar winds of O stars are clumped (e.g. B03). From the observational point of view, the possible wind clumping decreases the wind mass-loss rate inferred from the observation because the line profiles of clumped wind mimic those with higher mass-loss rate. According to the numerical simulations of wind instability (e.g. Feldmeier et al. 1997, Runacres & Owocki 2002) the theoretical mean mass-loss rate is nearly the same for smooth and structured winds. Thus, if the observations really show signatures of clumping at all spectral regions where the stellar wind is observed, then, according to our present knowledge, the theoretically predicted values of mass-loss rates should basically correspond to the values derived from observation with account of clumping. For our study we adopted the values derived from observations assuming "smooth" winds partly because these values were for larger SMC sample (to our knowledge) derived only by B03 and partly because the models of wind clumping are still schematic.

Wind parameters adopted for the comparison with theoretical values will be discussed individually for those stars, for which it is necessary. Note that in the text we will term the mass-loss rate estimated from observation as "observed mass-loss rate", although one should keep in mind that this quantity cannot be directly derived from spectra and that it is model-dependent.

NGC 346 WB 1 This is a multiple system (Heydari-Malayeri & Hutsemékers 1991). The terminal velocity derived for this system by P96 $v_{\infty} = 2650 \text{ km s}^{-1}$ is marked as uncertain due to the complexity of the absorption profile. P96 note that another possible value of the terminal velocity is $v_{\infty} = 2250 \text{ km s}^{-1}$. Prinja & Crowther (1998) obtained value of edge velocity (velocity at which the line profile meets the continuum level) as $v_{\text{edge}} = 2830 \text{ km s}^{-1}$ for N V lines. Using their derived approximate relation $v_{\infty} = 0.8v_{\text{edge}}$ we obtain terminal velocity $v_{\infty} = 2260 \text{ km s}^{-1}$. Thus, we adopted $v_{\infty} = 2250 \text{ km s}^{-1}$ as a value of the terminal velocity.

NGC 346 WB 4 The observed terminal velocity by P96 $v_{\infty} = 1550 \text{ km s}^{-1}$ is quoted as uncertain. The typical terminal velocity for stars of similar spectral type is higher, the terminal velocity calculated as twice the escape velocity (roughly suitable for SMC stars, B03) is 1900 km s^{-1} . Using approximate relation $v_{\infty} = 0.8v_{\text{edge}}$ of Prinja & Crowther (1998) and their measurement of edge velocity of C IV lines we obtain $v_{\infty} = 1950 \text{ km s}^{-1}$. Hence, we adopt this value of terminal velocity.

NGC 346 WB 6 The edge velocity obtained for this star by Prinja & Crowther (1998) $v_{\text{edge}} = 1925 \text{ km s}^{-1}$ is lower than the terminal velocity $v_{\infty} = 2250 \text{ km s}^{-1}$ derived by P96 or $v_{\infty} = 2300 \text{ km s}^{-1}$ by B03. This difference probably illustrates the fact that the correct determination of wind velocities for SMC is difficult due to their low wind density.

This star was independently studied by P96, who obtained slightly lower value of the effective temperature than B03 ($T_{\text{eff}} = 40\,000 \text{ K}$).

Table 2. Stellar and wind parameters of selected SMC stars. Stellar parameters (radius R_* , the effective temperature T_{eff} and the metallicity relative to the solar value Z/Z_{\odot}) were adopted either from Puls et al. (1996, hereafter P96), Bouret et al. (2003, hereafter B03), Massey et al. (2004, hereafter M04) and Martins et al. (2004, hereafter Mr04). For the stellar mass M we assume values derived using evolutionary tracks. For stars with metallicities denoted as B03 and Mr04 we adopted detailed abundance determinations from B03 and Mr04 for C, N, O, Si, S and Fe and $Z/Z_{\odot} = 0.2$ for other heavier elements. Observed wind parameters (i.e. the mass-loss rates \dot{M} and the wind terminal velocities v_{∞}) were also mostly taken from P96, B03, M04 and Mr04 (when available), however see the discussion for individual stars. Predicted values of wind parameters were derived by our code. For stars for which v_{∞} value is not given in the table authors provide only lower limits that is in agreement with our predicted value of v_{∞} .

Star	Stellar parameters					Mass loss rates \dot{M}		Terminal velocities v_{∞}		Source
	Sp.	R_* [R_{\odot}]	M [M_{\odot}]	T_{eff} [K]	Z/Z_{\odot}	observed [$M_{\odot} \text{ yr}^{-1}$]	predicted [$M_{\odot} \text{ yr}^{-1}$]	observed [km s^{-1}]	predicted [km s^{-1}]	
NGC 346 WB 1	O4III	23.3	95	42 000	0.2	$4.8 \cdot 10^{-6}$	$3.5 \cdot 10^{-6}$	2250	2240	P96
NGC 346 WB 4	O5.5V	14.2	53	42 000	0.2	$\leq 1 \cdot 10^{-7}$	$7.8 \cdot 10^{-7}$	1950	2200	P96
NGC 346 WB 6	O4V	11.2	40	41 500	B03	$2.7 \cdot 10^{-7}$	$3.5 \cdot 10^{-7}$	2300	2180	B03
NGC 346 MPG 368	O5.5V	10.6	38	40 000	B03	$1.5 \cdot 10^{-7}$	$1.8 \cdot 10^{-7}$	2100	2580	B03
NGC 346 MPG 113	O6V	7.8	33	40 000	B03	$3 \cdot 10^{-9}$	$4.8 \cdot 10^{-8}$		3370	B03
N81 #2	O6.5	7.9	31	40 000	Mr04	$\lesssim 10^{-8}$	$4 \cdot 10^{-8}$		2880	Mr04
AzV 75	O5III	25.4	92	40 000	0.2	$3.5 \cdot 10^{-6}$	$3.8 \cdot 10^{-6}$	2100	2120	M04
N81 #1	O7	10.3	34	38 500	Mr04	$\lesssim 10^{-8}$	$9 \cdot 10^{-8}$		2530	Mr04
AzV 26	O6I	27.5	86	38 000	0.2	$2.5 \cdot 10^{-6}$	$3.8 \cdot 10^{-6}$	2150	1850	M04
AzV 232	O7Ia	29.3	93	37 500	0.2	$5.5 \cdot 10^{-6}$	$4.1 \cdot 10^{-6}$	1400	1880	P96
AzV 207	O7V	11.0	33	37 000	0.2	$1 \cdot 10^{-7}$	$1.0 \cdot 10^{-7}$	2000	2060	M04
N81 #11	O7.5	6.9	23	37 000	Mr04	$\lesssim 10^{-9}$	$2 \cdot 10^{-8}$		2270	Mr04
N81 #3	O8.5	5.0	19	36 000	Mr04	$\lesssim 3 \cdot 10^{-9}$	$3 \cdot 10^{-9}$		2260	Mr04
AzV 238	O9III	15.5	37	35 000	0.2	$1.3 \cdot 10^{-7}$	$2.8 \cdot 10^{-7}$	1200	1830	P96
NGC 346 MPG 487	O6.5V	10.2	25	35 000	B03	$3 \cdot 10^{-9}$	$3.0 \cdot 10^{-8}$		2300	B03
AzV 469	O8.5II	21.2	38	32 000	0.2	$1.8 \cdot 10^{-6}$	$4.0 \cdot 10^{-7}$	2000	2010	M04
NGC 346 MPG 12	O9.7V	10.1	21	31 000	B03	$1 \cdot 10^{-10}$	$1.7 \cdot 10^{-8}$		1820	B03

AzV 232 Crowther et al. (2002) applied models with wind blanketing to study the stellar parameters of this star and obtained much lower value of the effective temperature than P96 ($T_{\text{eff}} = 32\,000$ K). However, we calculated wind parameters with this new determination of stellar parameters (i.e. the effective temperature, stellar mass, radius and abundances of C, N, O) and we obtained too low value of the mass loss rate ($\dot{M} = 9 \cdot 10^{-7} M_{\odot} \text{ yr}^{-1}$), much lower than the observed value. Also models of VKL predict with this new parameters about five times lower mass-loss rate than the observed value. Probably, this may be caused by the fact that this star has a very peculiar chemical composition ($Z(\text{C})/Z_{\odot}(\text{C}) = 0.07$, $Z(\text{O})/Z_{\odot}(\text{O}) = 0.1$, whereas $Z(\text{N})/Z_{\odot}(\text{N}) = 2.0$, Crowther et al. 2002) and abundances of other elements which are also important for driving of the stellar wind were not determined. Thus, to keep our sample more homogeneous, we used the stellar parameters derived by P96.

3.2 Comparison of calculated wind parameters with observation

In Fig. 1 we compare calculated wind terminal velocities for selected stars with observed values. While for some stars there is a very good agreement between observed and calculated terminal velocities, for some stars the agreement is worse. Before we will discuss this problem in a next section let us conclude, that derived scatter between observed and calculated wind terminal velocities is slightly higher than that for Galactic stars (see KK1).

Generally, it is difficult to assess the accuracy of determination of wind parameters. P96 state that due to the edge variability and contamination of the edges of wind absorption lines by underlying photospheric lines the terminal velocities should be regarded as accurate up to $\pm 10\%$. Taking this as a typical error of terminal velocity determination we conclude, that with exception of stars

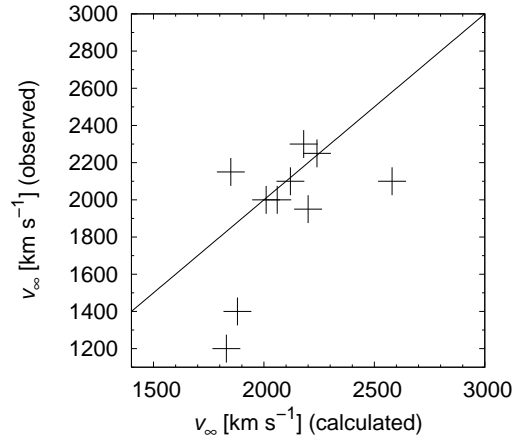


Figure 1. Comparison of calculated and observed terminal velocities. Stars for which there is no reliable estimate of their terminal velocities (in fact those stars that exhibit very weak winds) were excluded from the plot. Line denotes one to one relation.

NGC 346 MPG 368, AzV 26, AzV 232 and AzV 238 the rest of terminal velocity estimations lie within the mentioned uncertainty interval.

According to the predictions of stellar wind theory the wind terminal velocity v_{∞} is correlated with the surface escape velocity v_{esc} . For Galactic O stars the value of $v_{\infty}/v_{\text{esc}}$ does not depend on their effective temperature and has a mean value of about 2.5 (Lamers et al. 1995). Thus, we also plot the ratio of $v_{\infty}/v_{\text{esc}}$ for studied stars (see Fig. 2 where we compare ratio of $v_{\infty}/v_{\text{esc}}$ derived using theoretical and observed values of v_{∞}). The mean value of $v_{\infty}/v_{\text{esc}} \sim 2.3$ is slightly lower than that obtained by KK1 for

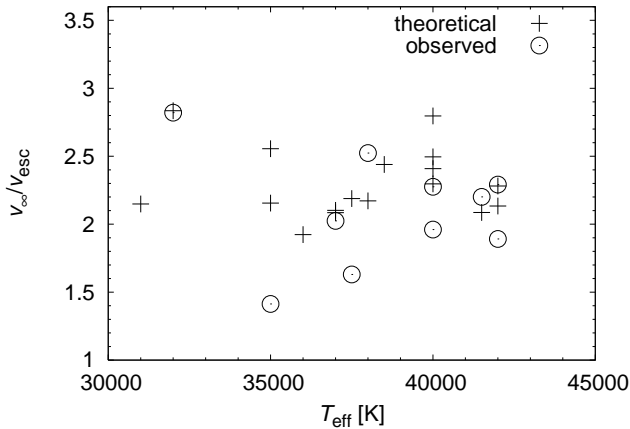


Figure 2. Comparison of the ratio of the wind terminal velocity v_∞ to the surface escape velocity v_{esc} derived using theoretical and observed values of v_∞ . Note that the observed values for stars with only lower limit of the terminal velocity available (missing v_∞ in Tab. 2) are not plotted in this graph.

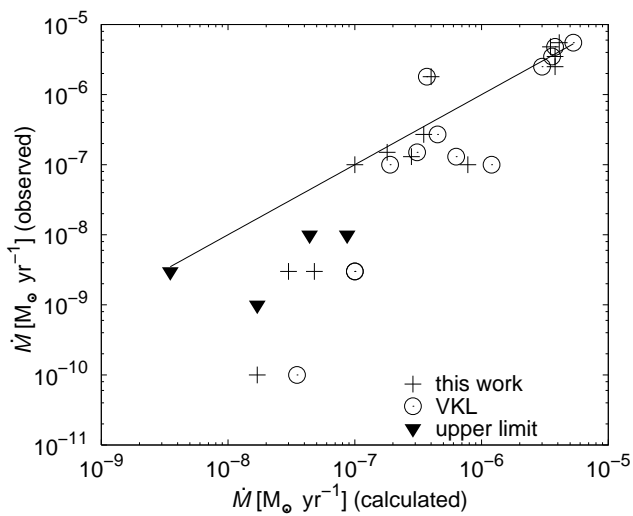


Figure 3. Comparison of calculated mass-loss rates (either by us or by VKL) and mass-loss rates derived from observation. Points corresponding to the upper limits were obtained using our model predictions and upper limits derived from observations. Line denotes one to one relation.

Galactic stars. Our calculated v_∞/v_{esc} ratio is slightly lower than recent observational finding of Evans et al. (2004), who derived the median $v_\infty/v_{\text{esc}} = 2.63$ for SMC stars with effective temperatures higher than 24 000 K. Since B03 obtained for their (however limited) sample $v_\infty/v_{\text{esc}} \sim 2.3$ we conclude that our calculations are in agreement with other studies and that our results may indicate that SMC hot stars terminal velocities are slightly lower than that of Galactic hot stars.

Similarly to Galactic O stars, there is a large scatter of both observed and theoretical v_∞/v_{esc} values (see Fig. 2). The scatter of theoretical values of v_∞/v_{esc} is slightly higher for SMC stars than for Galactic stars (KK1). The origin of this scatter is probably partly connected with high sensitivity of terminal velocities on detailed wind parameters in the outer wind regions (see Puls et

al. 2000 and also Sect. 4.3) and also with uncertain values of the terminal velocities.

The comparison of calculated mass-loss rates and mass-loss rates derived from observations in Fig. 3 shows relatively good agreement for stars with higher mass-loss rates ($\dot{M} \gtrsim 10^{-7} M_\odot \text{ yr}^{-1}$), in many cases better than for stars in our Galaxy (KK1). This is probably due to the fact that the distance to SMC is known with a relatively high precision and, thus, the basic stellar parameters are known also with a high precision (probably with exception of some systematic effects like wind blanketing effect which may influence parameters of both stellar groups). However, there is a significant disagreement between theoretical and observed values for lower mass-loss rates ($\dot{M} \lesssim 10^{-7} M_\odot \text{ yr}^{-1}$). In this case the predicted mass-loss rates are more than ten times higher than that derived from spectral analysis of observed data. This is not only a problem of our models, since also predictions of VKL show the same behaviour (see B03; Martins et al. 2004; 2005). To demonstrate this conclusion, we have added the mass-loss rate predictions of studied stars calculated using VKL recipe into Fig. 3. The possible origin of this discrepancy will be discussed in Sect. 5.

Our results for possible young Vz stars with thin winds ($\dot{M} \lesssim 10^{-7} M_\odot \text{ yr}^{-1}$) from Mr04 sample do not show that the systematic disagreement between predicted mass-loss rates and mass-loss rates derived from observation is higher than for generally older stars with thin winds from B03 sample (see Fig. 3).

For stars with very small mass-loss rates ($\dot{M} \lesssim 10^{-7} M_\odot \text{ yr}^{-1}$) only upper limits of their terminal velocities are available in the literature. Predicted terminal velocities of these stars are consistent with these upper limits. Note however that this is not a check of the models because the standard wind theory predicts that the terminal velocities and mass-loss rates are related – if the mass-loss rate of these stars is really much lower than the prediction derived in this paper, then their terminal velocities may be much higher.

The mass-loss rates derived by VKL recipe are slightly higher than that of us although KK1 found relatively good agreement between these theoretical rates. This is caused by a different boundary flux used. The line-blanketed fluxes from OSTAR2002 grid used in this work have lower flux in the UV domain (this domain is important for the line-driving) than H-He models used by KK1, consequently derived mass-loss rates are slightly lower. However, the effect of different boundary fluxes on terminal velocities is small.

3.3 Wind momentum-luminosity relationship

Wind momentum-luminosity relationship (see Kudritzki & Puls (2000) and references therein) may provide an independent method for the determination of stellar and consequently also galactic distances. However, to achieve this, detailed calibration of this relationship is necessary, especially with respect to the metallicity. Low-metallicity environment of SMC provides an ideal tool for such a calibration.

We compare theoretical modified wind momentum-luminosity relationship $\dot{M}v_\infty (R_*/R_\odot)^{1/2}$ obtained for considered stars using our NLTE wind models with a relationship derived from observations of these stars (see Fig. 4). We excluded observed values for stars for which only upper limits of their terminal velocities were derived from observation. We conclude that there is a relatively good agreement between calculated values and those derived from observation. Note however that the agreement for ex-

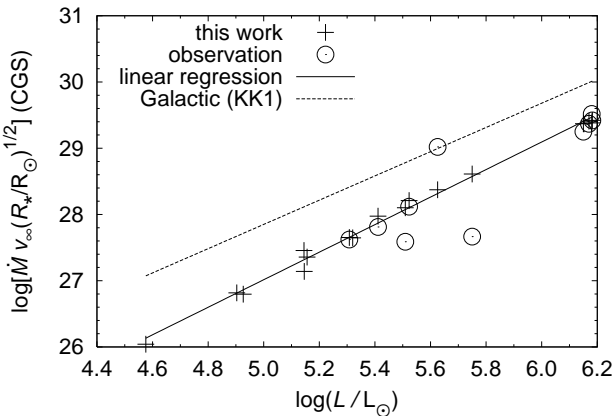


Figure 4. Comparison of calculated (crosses) and observed (circles) modified wind momentum for considered stars. Note that observed values for stars with unknown terminal velocity were excluded from this plot since it is possible to obtain at most only lower limits to their modified wind momentum (for stars with known observed mass-loss rates). Linear regression of calculated data of SMC and Galactic (KK1) stars is also plotted.

Table 3. Comparison of modified wind momentum-luminosity relationship (see Eq. (1)) taken from different sources. SMC denotes sample considered in this paper, either calculated from theoretical values or from values derived from observation (again excluding the observed values for stars with very weak winds).

Sample	$\log D_0$	x
Galactic (Vink et al. 2000)	18.68 ± 0.26	1.826 ± 0.044
Galactic (KK1)	18.7 ± 2.3	1.83 ± 0.40
SMC (theoretical)	16.6 ± 0.2	2.08 ± 0.04
SMC (observed)	16.6 ± 2	2.1 ± 0.4

cluded stars with unknown terminal velocity (for stars with $\dot{M} < 10^{-7} M_\odot \text{ year}^{-1}$) is very poor (using either lower limits of their terminal velocities or terminal velocities derived from our calculations), since their predicted mass-loss rates are much higher than the observed ones. On the other hand standard theory predicts that terminal velocities and mass-loss rates are related. In such a case the terminal velocities of these stars could be much higher and the agreement between predicted and observed wind momentum-luminosity relationship could be improved.

We have also calculated the linear regression of both theoretical and observed modified wind momentum-luminosity relationship for considered stars

$$\log [\dot{M} v_\infty (R_*/R_\odot)^{1/2}] = x \log(L/L_\odot) + \log D_0, \quad (\text{CGS}) \quad (1)$$

and compared it with the theoretical values derived for Galactic stars (Tab. 3). First, due to relatively good agreement of mass-loss rates there is a good agreement between theoretical and observed modified wind momentum-luminosity relationship for SMC stars (excluding stars with thin wind). Moreover, due to lower mass-loss rates of SMC stars the D_0 value is significantly lower than that for Galactic stars. Also the slope is slightly different. Roughly $5 - 6 \times$ lower modified wind momentum derived in the present study compared to that derived by KK1 for Galactic stars is mostly due to lower wind mass-loss rates caused by low metallicity of SMC

and to a lesser extent by a downward revision of mass-loss rates due to the use of blanketed model atmospheres.

4 INFLUENCE OF THE UNCERTAINTIES OF STELLAR PARAMETERS DETERMINATION

Individual stellar parameters (like the effective temperature, mass or radius) are not in some cases determined with a high degree of precision. This is especially true for hot stars for which large uncertainties of derived stellar radii (for Galactic stars due to uncertainties of the determination of their distance) and stellar masses (see Herrero et al. 1992, Lanz et al. 1996) may exist.

The uncertainties of determination of the stellar parameters influence also the predicted wind parameters (i.e. the mass-loss rates and the terminal velocities). To describe this in detail, we perform study of variations of predicted wind parameters with small change of stellar parameters. From the scaling of modified CAK theory (Kudritzki et al. 1989)

$$\dot{M} \sim N_0^{1/\alpha'} L^{1/\alpha'} [M(1 - \Gamma)]^{1-1/\alpha'}, \quad (2)$$

where N_0 is connected with number of lines that effectively drive the stellar wind, Γ is the Eddington parameter and

$$\alpha' = \alpha - \delta, \quad (3)$$

where α and δ are usual CAK parameters, so α' is typically equal to about 0.5. Hot star wind mass-loss rate mostly depends on the stellar luminosity L . With decreasing metallicity parameter N_0 decreases causing a decrease of mass loss rate. Finally, with decreasing effective mass $M(1 - \Gamma)$ mass loss rate increases. Since Eq. (2) does not take into account the variations of α' with e.g. the effective temperature, we also include the scaling of Vink et al. (2000) obtained for Galactic OB stars

$$\dot{M} \sim L^{2.2} M^{-1.3} T_{\text{eff}} (v_\infty/v_{\text{esc}})^{-1.3}, \quad (4)$$

with result of metallicity dependence derived by VKL as

$$\dot{M} \sim Z^{0.69}. \quad (5)$$

From the classical CAK theory it is known that the terminal velocity v_∞ depends mostly on the escape velocity v_{esc} (see Kudritzki & Puls (2000) for a review).

Here we do not aim to fit expressions like Eq. (2) for large amount of stars, however just to study variations of wind parameters with varying stellar parameters.

4.1 Effective temperature and stellar mass

Comparison of mass-loss rates and terminal velocities for studied stars calculated with original set of parameters and with stellar effective temperature by 1000 K higher is given in Fig. 5. Apparently, for higher effective temperature the mass-loss rate is higher, in agreement with other theoretical predictions (see Eqs. (2), (4)). From our calculations it is possible to derive that the mass-loss rate scales with the effective temperature as

$$\dot{M} \sim T_{\text{eff}}^{10.64}, \quad (6)$$

from which the effective parameter $\alpha' = 0.38$. This scaling is in a relatively good agreement with scaling of Vink et al. (2000, see Eq. (4)), which implies $\dot{M} \sim T_{\text{eff}}^{9.8}$. The dependence of the terminal velocity on the effective temperature (Fig. 5) is more scattered.

The variations of the mass-loss rate and the terminal velocity

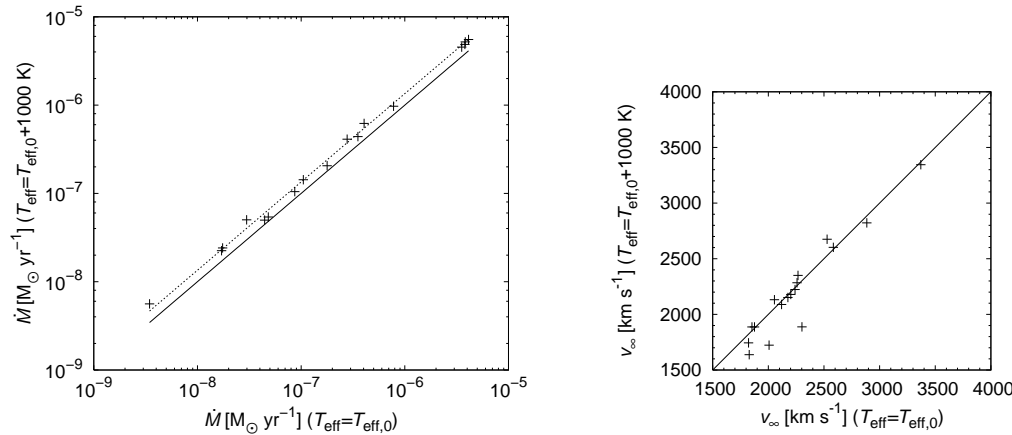


Figure 5. Comparison of the mass-loss rates (left panel) and the terminal velocities (right panel) of studied stars calculated with original effective temperature and effective temperature higher by 1000 K. Solid line denotes one to one relation and dashed line denotes linear fit to the relation between two groups of wind parameters.

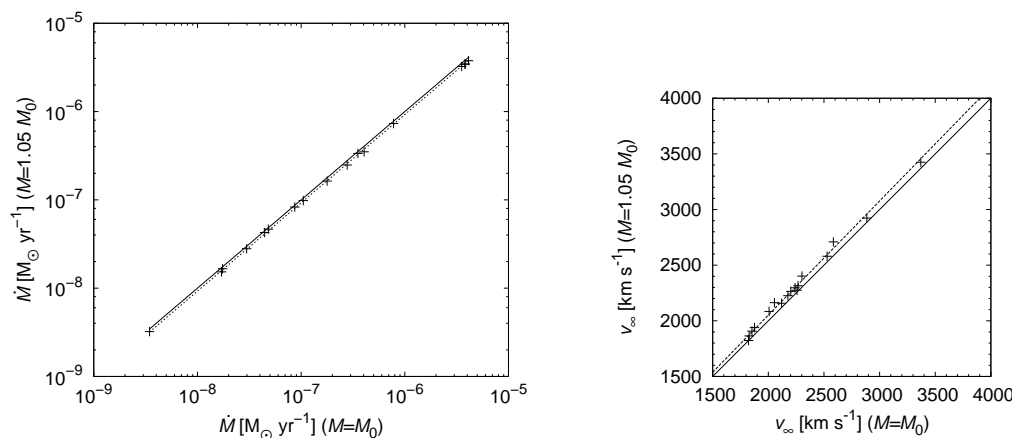


Figure 6. Comparison of the mass-loss rates (left panel) and the terminal velocities (right panel) of studied stars calculated with original mass and mass 1.05 times higher. Solid line denotes one to one relation and dashed line denotes linear fit to the relation between two groups of wind parameters.

with stellar mass are more stringent (Fig. 6). With increasing stellar mass the mass loss rate decreases, on average

$$\dot{M} \sim M^{-1.60}, \quad (7)$$

with fair agreement with Eqs. (2), (4) for the derived value $\alpha' = 0.38$. The terminal velocity is proportional to the escape velocity. From our calculations we derive the average relation

$$v_\infty \sim M^{0.52}, \quad (8)$$

which clearly reflects this proportionality.

It is clear that some part of the discrepancy between observed and theoretical wind parameters may be attributed to the uncertainties in the determination of the stellar parameters (mass and the effective temperature). Especially the downward revision of the stellar mass by the factor of $1.5 \times$ (e.g. due to the difference between spectroscopic and evolutionary masses) would cause downward revision of the terminal velocities by the factor of about 1.3 and the increase of the mass-loss rate by $2 \times$. On the other hand, since the distance to the SMC is known with a relatively high degree of precision we conclude that probably also another source of discrepancy between observed and predicted wind terminal velocities is present. Moreover, if higher terminal velocities scatter is given purely by

the uncertainties of determination of stellar mass and effective temperature, then similar effect should be also present in KK1, where slightly better agreement between theoretical and observed terminal velocities was derived.

4.2 Abundances

To study the variations of wind parameters with metallicity we recalculated wind models with the same stellar parameters as in Tab. 2, however with abundance of heavier elements 1.5 times higher. Comparison of the mass-loss rates and the terminal velocities calculated with different metallicities is given in Fig. 7.

For higher metallicity the radiative force is higher and consequently also the mass loss rate is higher. We have found that for studied stars the relation

$$\dot{M} \sim Z^{0.67} \quad (9)$$

holds. This is in a good agreement with VKL (see Eq. (5)).

The situation with the variations of the terminal velocity with the metallicity is more complicated. In Sect. 3.2 we concluded that the ratio of the wind terminal velocity to the stellar escape velocity v_∞/v_{esc} may be slightly higher for Galactic stars than for SMC

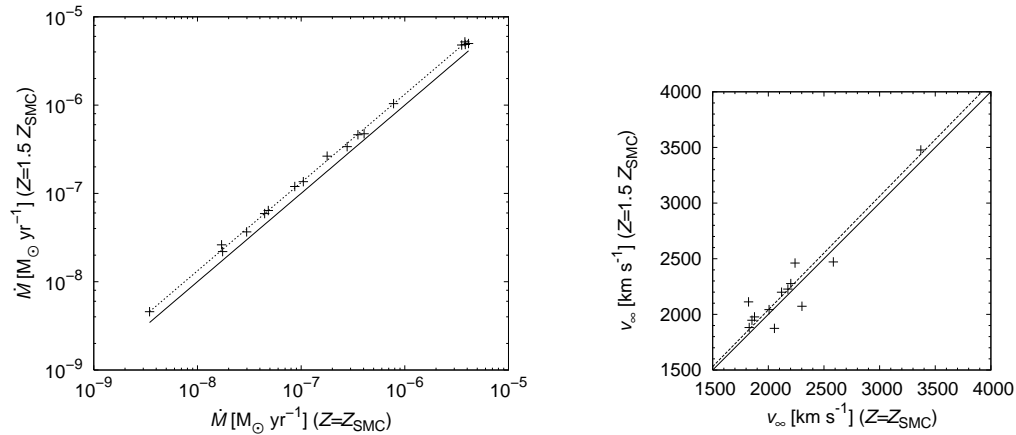


Figure 7. Comparison of the mass-loss rates (left panel) and the terminal velocities (right panel) of studied stars calculated with original metallicity and metallicity 1.5 times higher. Solid line denotes one to one relation and dashed line denotes linear fit to the relation between two groups of wind parameters.

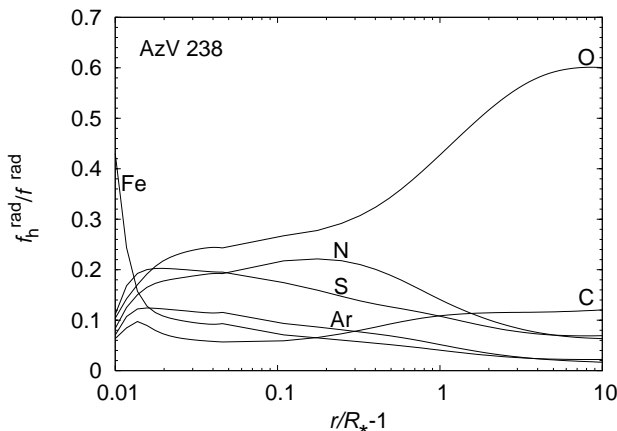


Figure 8. The radial variation of the contribution of the radiative force f_h^{rad} acting on element h to the total radiative force f^{rad} for star AzV 238 (plotted as $w_h^{\text{rad}} = f_h^{\text{rad}} / f^{\text{rad}}$). Iron is the most important element for the radiative driving close to the star, while oxygen dominates in the outer regions.

stars. With varying metallicity the wind density changes, consequently wind ionization and excitation state varies, and hence also terminal velocities of studied stars vary. However, these variations are not monotonic, as can be seen from Fig. 7. For some stars the terminal velocity does not significantly change with metallicity, for some of them increases, for some of them decreases. On average, the terminal velocity slightly increases with increasing metallicity for studied SMC stars,

$$v_\infty \sim Z^{0.06}. \quad (10)$$

From calculations of Kudritzki (2002) we can infer more steep proportionality, roughly $v_\infty \sim Z^{0.12}$.

4.3 Sensitivity of v_∞ on the conditions in the outer wind

Although *on average* the value of v_∞ depends on metallicity only slightly, the high scatter between terminal velocities derived using different metallicities in Fig. 7 may seem surprising. Similar effect was however, in a different context, reported also by other authors (e.g. Puls et al. 2000). The O star winds in the outer regions are accelerated mainly by few dozen lines of lighter elements (like C, N,

O, see Pauldrach 1987, Vink et al. 1999 and also Figs. 8 and 9). In such a case, the line acceleration is very sensitive to the detailed wind structure (i.e. temperature, density and chemical composition). Partly due to this, large variations of v_∞/v_{esc} (both observed and theoretical, see Lamers et al. 1995 and Pauldrach et al. 1990) occur for individual stars. This is also likely cause for the high scatter between terminal velocities derived using different metallicities in Fig. 7. This scatter also occurs when variations of terminal velocity with temperature (see Fig. 5) are studied. To a lesser extent this is also true for the variations of stellar mass, see Fig. 6.

The metallicity of studied stars is not known with a high precision. For many stars we used just scaled Galactic chemical composition, although significant deviations from this scaling exist (e.g. B03; they are also probably manifested by a different number ratio of WN to WC stars in the Clouds, see Mikulášek 1969). Moreover, we do not have any information on the abundance of many elements which are important for the radiative driving at all (e.g. Ne, Ar). Even worse, there are large differences in the chemical composition of individual stars (e.g. B03). To conclude, some part of higher scatter between observed and predicted terminal velocities can be attributed to poorly known chemical composition of most of the studied stars. Uncertainties of the determination of other stellar parameters, i.e. the stellar mass and the effective temperature may (besides the approximations involved in our code) also contribute to this scatter.

5 MULTICOMPONENT EFFECTS

Stellar winds of hot stars are accelerated mainly by the absorption of radiation in the resonance lines of heavier elements. The radiative acceleration acting on individual elements is however different, and consequently individual elements have different velocities. Consequently, stellar winds of hot stars have a multicomponent nature (e.g. Springmann & Pauldrach 1992, KKII). For many stars the velocity differences are small, thus the wind multicomponent nature can be neglected in this case. Krtička et al. (2003) showed that in the low-metallicity environment the velocity differences between wind components are larger, thus multicomponent effects are more important. However, as was noted e.g. by Mr04, even for relatively low-metallicity environment of stellar wind of SMC stars the multicomponent effects can be neglected.

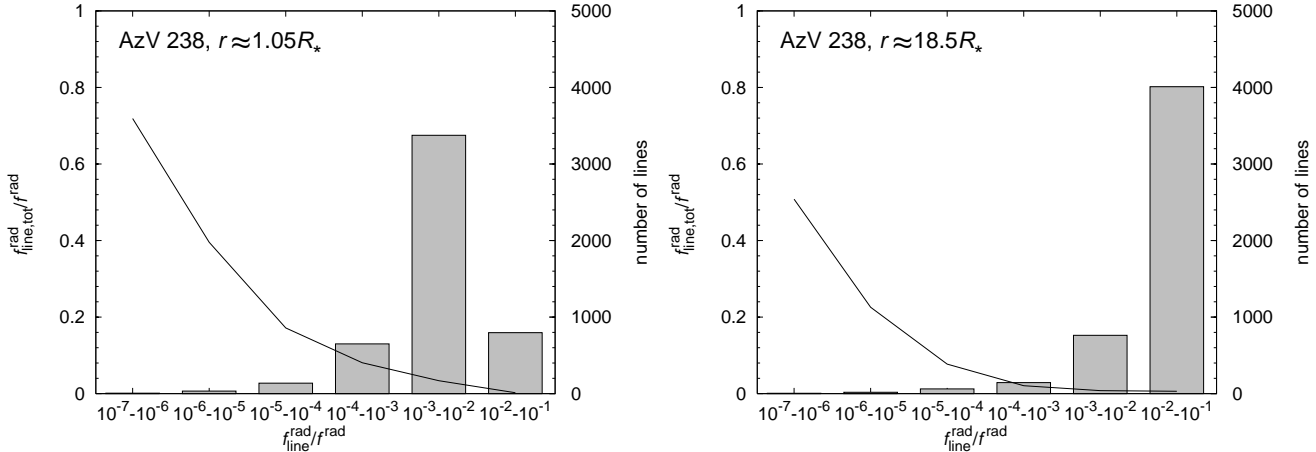


Figure 9. Contribution of lines with different strengths to the radiative force at the critical point ($r \approx 1.05R_*$, left panel) and in the outer wind region ($r \approx 18.5R_*$, right panel) for star AzV 238. The total relative contribution to the radiative force $f_{\text{line, tot}}^{\text{rad}}/f^{\text{rad}}$ summed over lines with given individual contribution to the radiative force $f_{\text{line}}^{\text{rad}}/f^{\text{rad}}$ is plotted using boxes. Solid line denotes number of spectral lines whose relative contribution to the radiative force lies in a given interval. Radiative acceleration close to the star is mainly due to hundreds of lines whose $f_{\text{line}}^{\text{rad}}/f^{\text{rad}}$ lies in the interval ($10^{-3} - 10^{-2}$), whereas the acceleration in the outer regions is given just by few dozens lines with $10^{-2} < f_{\text{line}}^{\text{rad}}/f^{\text{rad}} < 10^{-1}$.

On the other hand, these considerations are based on the assumption that the heavier elements can be described by one component only. By other words, usually it is assumed that atomic mass of heavier ions is the same, the radiative acceleration on heavier elements is the same and consequently these elements have the same mean velocity. However, in reality individual elements have different mass, the radiative acceleration acting on them is also different and consequently these elements have different mean velocities. Hence, multicomponent effects may occur for higher densities and metallicities than previously assumed.

5.1 Velocity differences in the stellar wind

To estimate the importance of multicomponent effects in the stellar wind of SMC stars we calculate approximate velocity differences between individual heavier elements h (accelerated by the line absorption) and passive wind component p (hydrogen and helium) using the momentum equation of individual wind elements. In the case of stationary spherically symmetric stellar wind this equation reads (cf. Burgers 1969, KKII)

$$v_{ra} \frac{dv_{ra}}{dr} = g_a^{\text{rad}} - g - \frac{1}{\rho_a} \frac{d}{dr} (a_a^2 \rho_a) + \frac{q_a}{m_a} E + \frac{1}{\rho_a} \sum_{b \neq a} K_{ab} G(x_{ab}) \frac{v_{rb} - v_{ra}}{|v_{rb} - v_{ra}|}, \quad (11)$$

where v_{ra} and ρ_a are the velocity and the density of component a ($a = p$ or $a = h$), a_a is the isothermal sound speed, E is the charge separation electric field, g is the gravitational acceleration, g_a^{rad} is the radiative acceleration and q_a and m_a are charge and mass of particle a . Frictional parameter has the following form:

$$K_{ab} = n_a n_b \frac{4\pi q_a^2 q_b^2}{k T_{ab}} \ln \Lambda, \quad (12)$$

where n_a and n_b are number densities of individual components and mean temperature of both components is

$$T_{ab} = \frac{m_a T_b + m_b T_a}{m_a + m_b} \quad (13)$$

(T_a and T_b are temperatures of wind components a and b) and $\ln \Lambda$ is the Coulomb logarithm. The argument of the Chandrasekhar function $G(x_{ab})$ is

$$x_{ab} = \frac{|v_{rb} - v_{ra}|}{\alpha_{ab}}, \quad (14)$$

where

$$\alpha_{ab}^2 = \frac{2k(m_a T_b + m_b T_a)}{m_a m_b}. \quad (15)$$

For low velocity differences ($x_{ab} \lesssim 1$) the flow is well coupled. However, for higher velocity differences ($x_{ab} \gtrsim 1$) the Chandrasekhar function is decreasing and this behaviour may enable dynamical decoupling of wind components (see Springmann & Pauldrach 1992, KKII).

In the momentum equation of heavier ions Eq. (11) the left-hand side term and the pressure term can be neglected. Also the gravitational acceleration and the electric polarisation field term can be neglected. Finally, due to high number density of passive component (hydrogen and helium) compared to the number density of heavier elements the only important frictional term is that between passive and other components. Consequently, the approximative momentum equation of heavier element h is

$$g_h^{\text{rad}} = \frac{1}{\rho_h} K_{hp} G(x_{hp}). \quad (16)$$

This equation states that whole momentum obtained by individual heavier elements due to the line-absorption is transferred by friction to the passive component. Using the Taylor expansion of the Chandrasekhar function (appropriate for $x_{hp} < 1$) $G(x_{hp}) \approx \frac{2x_{hp}}{3\sqrt{\pi}}$ the relative velocity difference between passive component and a given heavier ion h is

$$x_{hp} = \frac{|v_{rp} - v_{rh}|}{\alpha_{hp}} \approx g_h^{\text{rad}} \frac{m_h}{n_p} \frac{3kT}{8\sqrt{\pi} q_h^2 q_p^2 \ln \Lambda}, \quad (17)$$

where we have assumed $T_p \approx T_h \approx T$. For our discussion the relevant quantity is not the radiative acceleration g_h^{rad} itself, however the radiative force $f_h^{\text{rad}} = \rho_h g_h^{\text{rad}}$ (per unit volume). Thus,

$$x_{hp} \approx f_h^{\text{rad}} \frac{1}{n_h n_p} \frac{3kT}{8\sqrt{\pi} q_h^2 q_p^2 \ln \Lambda}. \quad (18)$$

The work done by the radiative acceleration is used to lift the wind material from the stellar gravitational well. Thus, for stars with the same mass-loss rates (and the same velocity field) the radiative force (at corresponding radii) shall be similar. These stars with lower metallicities have lower n_h and consequently higher x_{hp} . In reality, stars with lower metallicities have also lower mass-loss rates, lower n_p and consequently even higher x_{hp} . Due to these two effects (see also Krtička et al. 2003) stars with lower metallicities have higher velocity differences between wind components. The crucial point is, however, that heavier elements which are not abundant in the stellar wind (i.e. $n_h \ll n_p$) and which significantly contribute to the radiative acceleration (i.e. their f_h^{rad} is large) may have large relative velocity differences x_{hp} , in many cases $x_{hp} \approx 1$. In such a case, instability connected with the decoupling of considered element may occur.

Let us first roughly estimate in which situation this may occur. Let be w_h^{rad} the relative contribution of a given element h to the total radiative force f^{rad} , i.e.

$$f_h^{\text{rad}} = w_h^{\text{rad}} f^{\text{rad}}. \quad (19)$$

Neglecting the gravity, the pressure term and the electric polarisation field the total radiative force can be approximated from the momentum equation Eq. (11) of passive component as

$$f^{\text{rad}} \approx \rho_p v_r \frac{dv_r}{dr}, \quad (20)$$

where v_r is the mean wind velocity, we may assume $v_r \approx v_{rp}$. The velocity gradient can be estimated as

$$v_r \frac{dv_r}{dr} \approx \frac{v_\infty^2}{R_*}, \quad (21)$$

for n_h we can write from the approximate continuity equation

$$n_h \approx Z_h \frac{\dot{M}}{4\pi R_*^2 v_\infty m_h}, \quad (22)$$

where Z_h is the density of a given element relative to the bulk density ρ in the stellar atmosphere ($\rho_h = Z_h \rho$). Consequently using Eqs. (18)–(22) we derive

$$x_{hp} \approx w_h^{\text{rad}} v_\infty^3 R_* \frac{m_p m_h}{Z_h \dot{M}} \frac{3\sqrt{\pi k T}}{2q_h^2 q_p^2 \ln \Lambda}. \quad (23)$$

In the case when the heavier ions are approximated by one component only, we have $w_h^{\text{rad}} = 1$ and we arrive at Eq. (6) of Krtička et al. (2003). However, in many cases the abundance of individual element Z_h is much lower than \mathfrak{Y}_i (the ratio of total density of heavier "absorbing" ions and passive component in the atmosphere) and thus, predicted velocity differences are larger. Eq. (23) can be also rewritten in a more convenient form as

$$x_{hp} \approx 0.015 w_h^{\text{rad}} v_\infty^3 R_{12} \frac{A_h}{Z_h \dot{M}_{-11}} \frac{T_4}{z_h^2 z_p^2}, \quad (24)$$

where we have assumed $m_p = m_H$, $q_p = e z_p$, $q_h = e z_h$ and $m_h = A_h m_H$, where e is the elementary charge and m_H is the proton mass, and scaled quantities are $\dot{M}_{-11} \equiv \dot{M}/(10^{-11} M_\odot \text{yr}^{-1})$, $v_\infty \equiv v_\infty/(10^8 \text{cm s}^{-1})$, $R_{12} \equiv R_*/(10^{12} \text{cm})$, and $T_4 \equiv T/(10^4 \text{K})$. From Eq. (24) it follows that for heavier elements ($A_h \approx 10$) with low abundance ($Z_h \approx 10^{-5}$) which significantly contribute to the radiative force (i.e. $w_h \approx 0.1$) the decoupling ($x_{hp} \gtrsim 1$) can occur for relatively large mass-loss rates (of order $10^{-8} M_\odot \text{yr}^{-1}$). The mass-loss rate for which the decoupling occurs in the winds of SMC stars is approximately five times higher than the mass-loss rate for which the decoupling occurs in the winds of Galactic stars, since $Z_{h, \text{SMC}} \approx 0.2 Z_{h, \odot}$.

Eq. (24) provides only a very approximate expression for the velocity difference, mainly due to a very simplified velocity gradient assumed in Eq. (21). For a more reliable estimate it is much better to use Eq. (18).

Note that this picture of decoupling is somehow different from that presented by other studies, i.e. Springmann & Pauldrach (1992) and KKII and discussed by Mr04. These studies assumed that all heavier ions which are accelerated by line-transitions decouple from the mean (passive) flow. However now we discuss a more realistic description that individual ions decouple from the mean flow separately.

5.2 Velocity differences in the winds of studied SMC stars

We used our NLTE wind code to calculate approximative velocity differences in studied SMC stellar winds. For this purpose we applied Eq. (18), where both the contribution of a given element to the radiative force w_h and charges of wind components q_h and q_p are calculated using our NLTE wind code.

Calculated values of x_{hp} for individual stars and individual elements are given in Fig. 10. Generally, the relative velocity differences are smallest close to the star, where the stellar wind is relatively dense. As the stellar wind accelerates, the wind density is lower and velocity differences are higher. At some point the velocity differences have its maximum and for larger radii decrease outwards due to decreasing velocity gradient. This general behaviour of relative velocity differences was described elsewhere (KKII). In our case the behaviour is more complicated mainly due to the processes of ionization and recombination.

For most of the stars and for most of the elements the velocity differences are rather low, $x_{hp} \ll 1$, thus there occurs no decoupling in this case. However, in some cases, especially in those where the wind density is low, the relative velocity difference between argon (or sulphur) and passive component becomes higher and close to one. This is caused by the fact that argon and sulphur have very low metallicity ($Z_{\text{Ar, SMC}} \approx 3 \cdot 10^{-5}$) and significantly contribute to the radiative force ($w_{\text{Ar}}^{\text{rad}} \approx 0.1$). The velocity differences are so high, that they may cause large frictional heating.

5.3 Multicomponent wind models

To test the possibility of frictional heating, we have calculated four-component wind models, where the fourth component is either argon, sulphur or carbon, depending on which element for a given star has a maximum velocity difference. The other three components are heavier ions, passive component (hydrogen and helium) and free electrons.

First, we tested whether the simple equation Eq. (18) is able to reliably predict the velocity differences. We plot the result only for the case of star NGC 346 WB 1 (see Fig. 11), however the result that Eq. (18) is able to very reliably predict the approximate velocity differences is similar also for other stars.

For stars with highest velocity differences the frictional heating occurs¹. This is shown in Figs. 12, 13, where we compare

¹ In the common case that occurs in the stellar atmosphere and wind it is usually not necessary to differentiate between kinetic temperatures of individual particles since these temperatures are nearly equal. However, in the present case the temperatures of individual wind components significantly differ. Since the collisional terms that enter into the statistical equilibrium equations are caused by the collisions with free electrons that move with

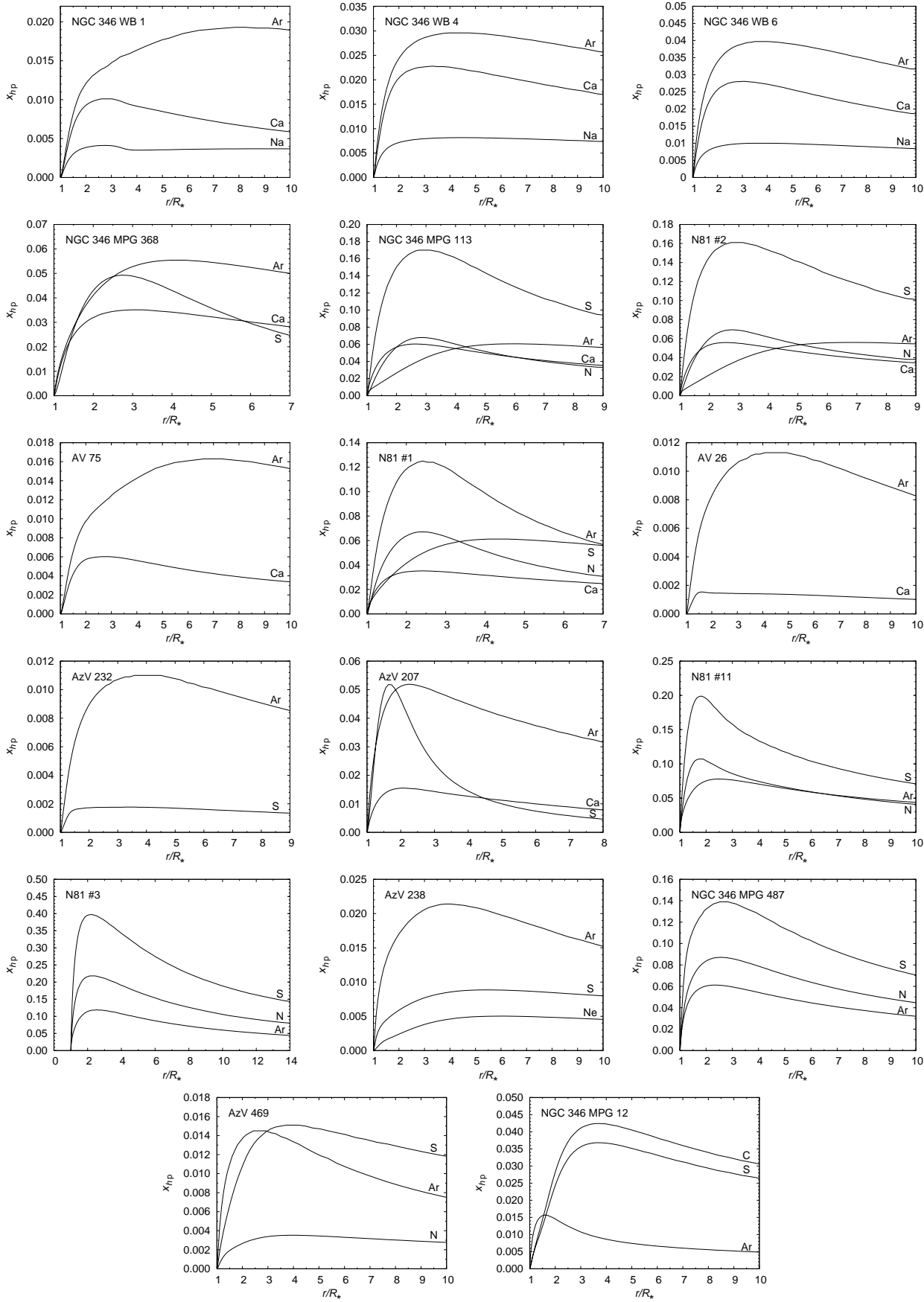


Figure 10. Relative velocity differences between individual heavier elements and passive component calculated using Eq. (18). Only values for elements with highest relative velocity differences are plotted. Velocity differences for other heavier elements are much lower.

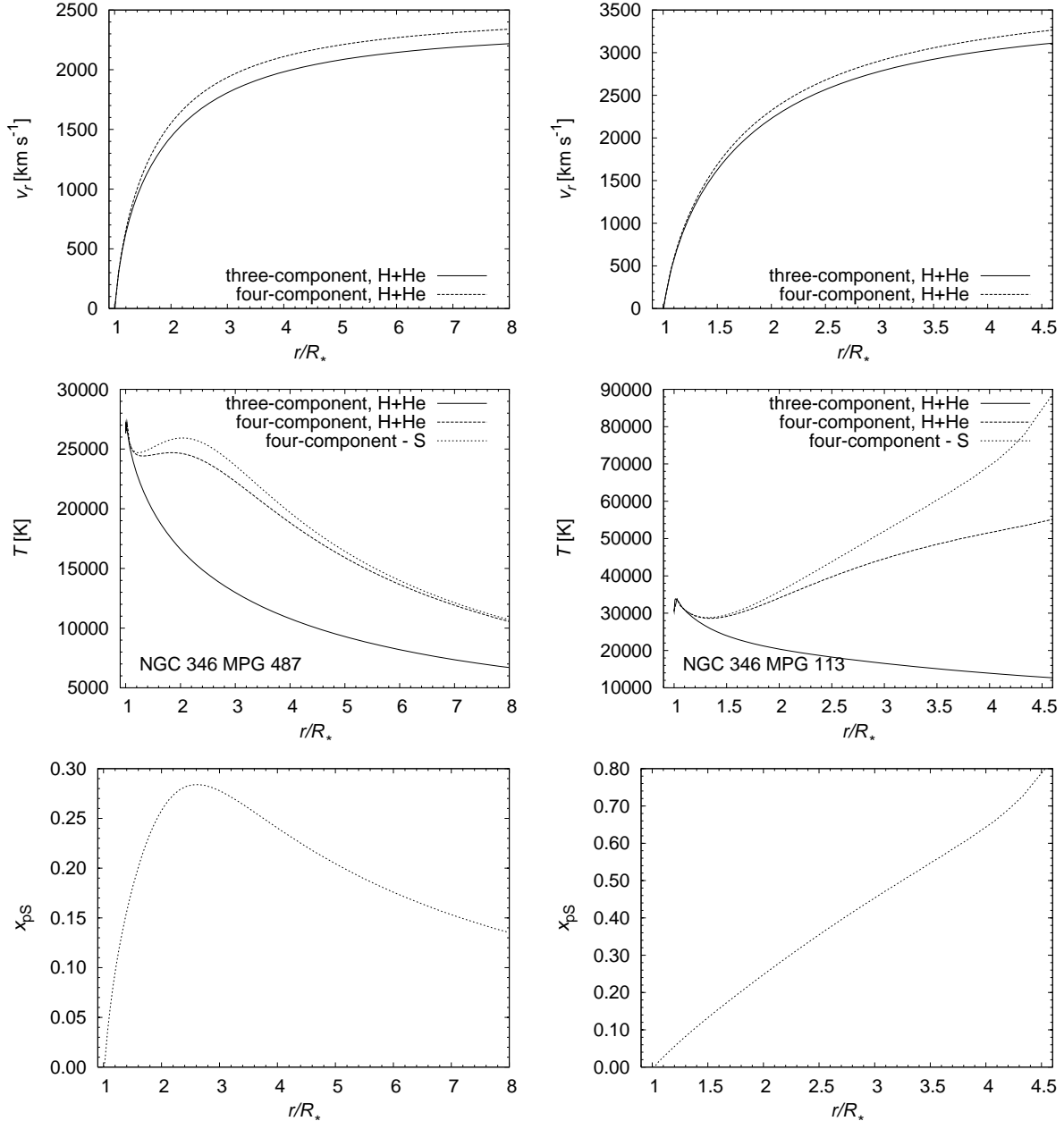


Figure 12. Comparison of four-component model (with sulfur as a fourth component, dashed line) and three-component model (solid line) for star NGC 346 MPG 487 (left) and NGC 346 MPG 113 (right). *Top panel:* Comparison of velocity of passive component (hydrogen+helium) in individual models. Note that the velocities of all individual wind components in four-component or three-component models are similar. *Middle panel:* Comparison of wind temperatures. Wind temperatures of individual wind components in three-component model are nearly equal. Wind temperature in four-component model is higher due to the frictional heating and sulfur temperature is even higher than the temperature of other components. *Bottom panel:* Relative velocity difference between passive component and sulphur in four-component model. The velocity difference in the case of NGC 346 MPG 113 is close to one in the outer wind regions, thus potentially enabling instability due to sulphur decoupling.

four-component models (with wind components sulphur, remaining heavier ions, passive component and electrons) with three-component models (with wind components heavier ions, passive component and electrons). In the outer wind regions the relative

much higher thermal speed than other particles, we inserted the electron temperature into all terms in the statistical equilibrium equations. This is indeed only approximative in the case of relatively large velocity differences between wind components.

velocity difference between passive component and sulphur x_{ps} is close to 1. Due to this higher velocity difference the stellar wind is frictionally heated in the outer parts. Consequently, wind temperature is higher in four-component model than in three-component one. Higher wind temperature also slightly modifies the radiative force since wind velocity is slightly higher in four-component case.

The frictional heating also slightly modifies the ionization equilibrium. The ionization fraction of higher ionization stages (such as N V, O V) of frictionally heated wind is higher than in

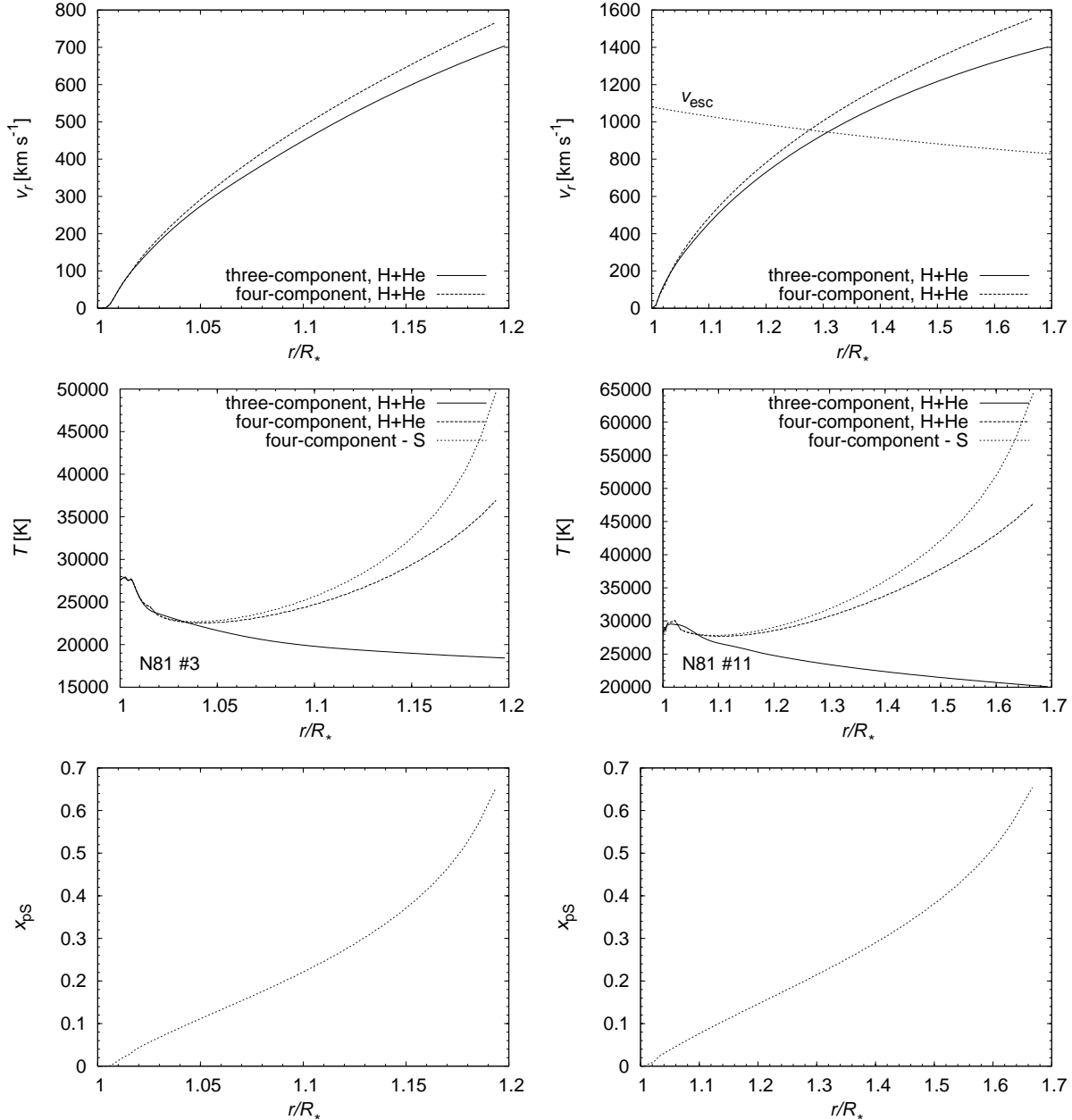


Figure 13. The same as Fig. 12 for SMC-N81 stars #3 (left) and #11 (right). Note that for winds of both stars the friction between sulphur and passive wind component (hydrogen and helium) is important for wind structure. In both cases the sulphur decoupling may occur. In the case of SMC-N81 #3 sulphur may decouple for velocities lower than the escape speed (the surface escape speed for this star is $v_{\text{esc}} = 1180 \text{ km s}^{-1}$) and in the case of SMC-N81 #11 sulphur may decouple for velocities slightly higher than the escape speed (the escape speed is also plotted on the graph of this star).

the wind with negligible frictional heating, whereas the ionization fractions of lower ionization stages (e.g. C IV, Si IV) are lower in the frictionally heated wind. The differences are by about a factor of 2.

The velocity differences in the case of frictionally heated four-component wind models are larger than those estimated using approximate Eq. (18) (cf. Fig. 10), since velocity difference increases with increasing temperature. The velocity difference in the case of NGC 346 MPG 113, SMC-N81 #11 and #3 is so high that the wind instability connected with sulphur decoupling may occur (Owocki & Puls 2002, Krtička & Kubát 2002). For star #3 this occurs for velocities lower than the escape speed.

We have shown that for stars that have very low observed mass-loss rates the velocity differences for some heavier elements are high. In such case either frictional heating becomes important or even some elements may decouple from the wind. Note that these multicomponent effects are important already for theoretically derived mass-loss rates, i.e. those that are much higher than the observed ones. Since the frictional heating increases the wind temperature only in the outer wind regions (for velocities higher than that corresponding to the critical point velocity), its influence on the mass-loss rate is negligible.

Fall back of the wind material (which may cause the lowering of wind mass-loss rate) may occur only if the wind components de-

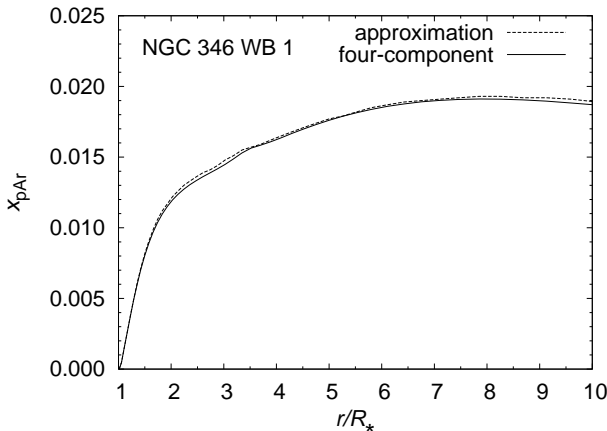


Figure 11. Comparison of relative velocity differences between passive component and argon calculated using approximate expression Eq.(18) and using four-component model. Clearly, in the case of negligible frictional heating Eq.(18) is able to correctly predict velocity differences.

couple below the point where wind velocity is equal to the escape velocity. Only in this case the runaway instability connected with decoupling may lead to fall back of wind material (Porter & Skoruza 1999, Votruba et al. 2006) and consequently lower the mass-loss rate. This occurs only for star SMC-N81 #3. For other stars we have not obtained the possibility of decoupling close to the stellar surface, for velocities lower than the escape velocity. This means that presented models are, with one exception, close to the star stable for perturbations of multicomponent flow. Consequently, we are not able to explain very low observed mass-loss rates using multicomponent models for all except one star. Only for star SMC-N81 #3 the low observed mass-loss rate may be connected with multicomponent effects.

6 DISCUSSION AND CONCLUSIONS

We have presented NLTE wind models of cooler O stars in SMC. These models enable prediction of basic wind parameters, i.e. the mass-loss rates and the terminal velocities. We have compared these predicted wind parameters with those derived from observation. We have concluded that there is a relatively good agreement between observed and predicted terminal velocities with some scatter. This scatter can be partly attributed to the poorly known chemical composition of SMC stars. Moreover, the existence of unidentified binaries in our sample can also influence the comparison. Last but not least, the simplification involved in our code (e.g. simplified treatment of radiative transfer equation, like neglect of line overlaps) can also influence the results. However, the situation with mass-loss rates is different. For relatively high mass-loss rates (i.e. $\dot{M} \gtrsim 10^{-7} M_\odot \text{ yr}^{-1}$) there is again a good agreement between predicted quantities and those derived from observations. However, for smaller mass-loss rates the agreement is rather poor, predicted mass-loss rates are significantly higher than those derived from observation. Note that this is not an effect of our models only, since there is a similar disagreement between observations and models of VKL (see B03 and Mr04).

We have tested whether the mentioned systematic disagreement between theoretical and observed values of mass-loss rates can be caused by the decoupling of some metals from the mean flow. We have shown that for stars with relatively good agreement

between observed and predicted mass-loss rates the velocity differences are small (and thus there is no decoupling of wind components). On the other hand for stars for which the predicted mass-loss rates are systematically too high either the instability connected with the decoupling of wind components may occur or the frictional heating increases wind temperature. Note however that only for one star we have obtained the possibility of decoupling close to the stellar surface for velocities lower than the escape velocity. (Note that in order to obtain fall back of the wind material and consequently lower wind mass-loss rate it is necessary to the decoupling occur below the point where wind velocity is equal to the escape velocity.) With this exception, presented models are, to our knowledge, close to the star stable for perturbations of multicomponent flow. This means that we are not able without any further assumptions to explain very low observed mass-loss rates of most studied stars with $\dot{M} \lesssim 10^{-7} M_\odot \text{ yr}^{-1}$ (although in the outer wind regions of these stars the multicomponent effects are important). However, there are several possibilities how to (from the theoretical point of view) obtain decoupling of wind components for the velocities lower than the escape velocity also for other stars (like slightly different metallicity, overestimation of theoretical mass-loss rates, neglect of some heavier elements or improved treatment of the multicomponent flow). Another way how to explain low wind mass-loss rates may be connected with the thin-wind effect (Puls et al. 1998, Owocki & Puls 1999).

The decoupling discussed here slightly differs from that studied so far (cf. Springmann & Pauldrach 1992, KKII). In the previous studies it was usually assumed that metals and passive component may decouple completely. We present here a more detailed and more realistic picture of the decoupling of wind components. We showed that some elements which have very low abundance, however which significantly contribute to the radiative force, may decouple (or cause the instability connected with the decoupling) individually from the mean flow, that is basically not decoupled. Moreover, the decoupling may occur for higher mass-loss rates than it was previously assumed. We present an approximate formula for the test of importance of discussed decoupling of individual heavier elements.

For our comparison we used mass-loss rates derived from the observation assuming smooth winds. If the O star winds are clumped, as is indicated by observations of e.g. B03 or Martins et al. (2005), then the mass-loss rates of O stars are likely lower than predicted by current hot star wind theory and we obtain a disagreement between observations and theory for all stars. On the other hand a better treatment of the opacity sources in the UV domain with account of the line overlaps and comoving-frame radiative transport may help to overcome this potential disagreement.

We have studied the dependence of wind parameters on metallicity. It is well-known that the mass-loss rate increases with increasing metallicity. We have derived that the mass-loss rate scales with metallicity as $\dot{M} \sim Z^{0.67}$. The terminal velocity of individual stars also varies with metallicity mainly due to the sensitivity of the radiative force on detailed wind state in outer wind regions. However, on the average the terminal velocity varies with metallicity only slightly (for studied values of metallicity) as $v_\infty \sim Z^{0.06}$. As a consequence, the ratio of wind terminal velocity to the surface escape velocity $v_\infty/v_{\text{esc}} \sim 2.3$ is only slightly lower than for Galactic stars.

ACKNOWLEDGEMENTS

The author would like to thank Dr. Joachim Puls for valuable comments on the manuscript and to Drs. Jiří Kubát and Zdeněk Mikulášek for the discussion of this topic. This research has made use of NASA's Astrophysics Data System and the SIMBAD database, operated at CDS, Strasbourg, France. This work was supported by grants GA ČR 205/03/D020, 205/04/1267.

REFERENCES

Abbott D. C., 1982, *ApJ*, 259, 282

Bouret J.-C., Lanz T., Hillier D. J. et al., 2003, *ApJ*, 595, 1182 (B03)

Bautista M. A., 1996, *A&AS*, 119, 105

Bautista M. A., & Pradhan A. K., 1997, *A&AS*, 126, 365

Burgers J. M., Flow equations for composite gases, Academic Press, New York 1969

Butler K., Mendoza C., & Zeippen C. J., 1993, *J. Phys. B.*, 26, 4409

Castor J. I., 1974, *MNRAS* 169, 279

Castor J. I., Abbott D. C., & Klein R. I., 1975, *ApJ*, 195, 157 (CAK)

Charbonnel C., Meynet G., Maeder A., Schaller G., & Schaerer D., 1993, *A&AS*, 101, 415

Chen G. X., & Pradhan A. K., 1999, *A&AS*, 136, 395

Crowther P. A., Hillier D. J., Evans C. J., et al., 2002, *ApJ*, 579, 774

Evans C. J., Lennon D. J., Trundle C., Heap S. R., & Lindler D. J., 2004, *ApJ*, 607, 451

Feldmeier A., Puls J., & Pauldrach, A. W. A., 1997, *A&A*, 322, 878

Gräfener G., & Hamann W.-R., 2005, *A&A*, 432, 633

Herrero A., Kudritzki R. P., Vilchez J. M., et al., 1992, *A&A*, 261, 209

Heydari-Malayeri M., & Hutsemékers D., 1991, *A&A*, 243, 401

Hillier D. J., & Miller D. L., 1998, *ApJ*, 496, 407

Hubeny I., 1988, *Comput. Phys. Commun.*, 52, 103

Hubeny I., & Lanz T., 1992, *A&A*, 262, 501

Hubeny I., & Lanz T., 1995, *ApJ*, 439, 875

Hummer D. G., Berrington K. A., Eissner W., et al., 1993, *A&A*, 279, 298

Hubeny I., in *Stellar Atmosphere Modelling I*. Hubeny D. Mihalas & K. Werner eds., ASP Conf. Ser., Vol. 288, 17

Krtička J., & Kubát J., 2001, *A&A*, 377, 175 (KKII)

Krtička J., & Kubát J., 2002, *A&A*, 388, 531

Krtička J., & Kubát J., 2004, *A&A*, 417, 1003 (KK1)

Krtička J. & Kubát J., 2005, in *The A-Star Puzzle*, IAU Symposium No. 224 J. Zverko W.W. Weiss J. Žižňovský & S.J. Adelman, eds., 23

Krtička J., Owocki S. P., Kubát J., Galloway R. K., & Brown J. C., 2003, *A&A*, 402, 713

Kubát J., 1993, PhD. thesis, Astronomický ústav AV ČR, Ondřejov

Kubát J., 2003, in *Modelling of Stellar Atmospheres*, IAU Symp. 210 N. E. Piskunov W. W. Weiss & D. F. Gray eds., ASP Conf. Ser., A8

Kubát J., Puls J., & Pauldrach A. W. A., 1999, *A&A*, 341, 587

Kudritzki R. P., Pauldrach A. W. A., & Puls J., 1987, *A&A*, 173, 293

Kudritzki R. P., Pauldrach A. W. A., Puls J., & Abbott D.C., 1989, *A&A*, 219, 205

Kudritzki R. P., & Puls J., 2000, *ARA&A*, 38, 613

Kudritzki R. P., 2002, *ApJ*, 577, 389

Kupka F., Piskunov N. E., Ryabchikova, T. A., Stempels H. C., & Weiss W. W., 1999, *A&AS*, 138, 119

Lamers H. J. G. L. M., Snow T. P., & Lindholm D. M., 1995, *ApJ*, 455, 269

Lanz T., de Koter A., Hubeny I., & Heap S. R., 1996 *ApJ*, 465, 359

Lanz T., & Hubeny I. 2003, *ApJS*, 146, 417

Luo D., & Pradhan A. K., 1989 *J. Phys. B*, 22, 3377

Martins F., Schaerer D., Hillier D. J., & Heydari-Malayeri M., 2004, *A&A*, 420, 1087 (Mr04)

Martins F., Schaerer D., Hillier D. J., 2005, *A&A*, 436, 1049

Massey P., Bresolin F., Kudritzki R. P., Puls J., & Pauldrach A. W. A., 2004, *ApJ*, 608, 1001 (M04)

Mihalas D., & Hummer D. G., 1974, *ApJS* 28, 343

Mikulášek Z., 1969, *BAICz*, 20, 215

Nahar S. N., & Pradhan A. K., 1996, *A&AS*, 119, 509

Nahar S. N., & Pradhan A. K., 1993 *J. Phys. B*, 26, 1109

Ng K. C. J. *Chem. Phys.*, 61, 2680

Owocki S. P., & Puls J., 1999, *ApJ*, 510, 355

Owocki S. P., & Puls J., 2002, *ApJ*, 568, 965

Pauldrach A. W. A., 1987, *A&A*, 183, 295

Pauldrach A. W. A., Hoffmann T. L., & Lennon, M., 2001 *A&A*, 375, 161

Pauldrach A. W. A., Kudritzki R. P., Puls, J., & Butler K., 1990, *A&A*, 228, 125

Piskunov N. E., Kupka F., Ryabchikova T. A., Weiss, & W. W., Jeffery C. S., 1995, *A&AS*, 112, 525

Porter J. M., & Skouza B. A., 1999, *A&A*, 344, 205

Prinja R. K., & Crowther P. A., 1998, *MNRAS*, 300, 828

Puls J., Kudritzki R.-P., Herrero A., et al., 1996, *A&A*, 305, 171 (P96)

Puls J., Springmann U., & Lennon M., 2000, *A&AS*, 141, 23

Puls J., Springmann U., & Owocki S. P., 1998, in *Cyclical Variability in Stellar Winds* L. Kaper and A. W. Fullerton eds., Springer-Verlag, 389

Runacres M. C., & Owocki S. P., 2002, *A&A*, 381, 1015

Rybicki G. B. & Hummer D. G., 1992, *A&A*, 262, 209

Sawey P. M. J., & Berrington K. A., 1992, *J. Phys. B*, 25, 1451

Seaton M. J., 1987 *J. Phys. B*, 20, 6363

Seaton M. J., Zeippen C. J., Tully J. A., et al., 1992, *Rev. Mexicana Astron. Astrofis.*, 23, 19

Sobolev V. V. 1947, *Dvizhushchiesia obolochki zvezd*, Leningrad. Gos. Univ., Leningrad

Springmann U. W. E., & Pauldrach A. W. A., 1992, *A&A*, 262, 515

Venn K. A., 1999, *ApJ*, 518, 405

Vink J. S., de Koter A., & Lamers, H. J. G. L. M., 1999, *A&A*, 350, 181

Vink J. S., de Koter A., & Lamers, H. J. G. L. M., 2000, *A&A*, 362, 295

Vink J. S., de Koter A., & Lamers, H. J. G. L. M., 2001, *A&A*, 369, 574 (VKL)

Votruba V., Feldmeier A., Kubát J., & Nikutta R., 2006, in *Active OB-Stars: Laboratories for Stellar & Circumstellar Physics*, S. Štefl, S. Owocki and A. Okazaki eds

Zhang H. L., 1996, *A&AS*, 119, 523

Zhang H. L., & Pradhan A. K., 1997, *A&AS*, 126, 373